Lasers in Manufacturing Conference 2025

Towards optimized 2.5D ultra-short pulsed laser ablation of fused silica to enhance quality of laser structured complex optics

Dominik Mücke[a]*, Cemal Esen[b], Ralf Hellmann[a]

[a] *Applied Laser and Photonics Group, University of Applied Sciences Aschaffenburg, Würzburger Str. 45, 63739 Aschaffenburg, Germany*
[b]*Applied Laser Technologies, Ruhr-University Bochum, Universitätsstraße 150, 44801 Bochum*

Abstract

Ultrafast laser ablation has been proven to allow for the generation of micromechanical devices, micro-optics and microfluidics. To successfully transfer this approach towards an industrial level, process efficiency and stability as well as resulting parts quality have to be improved. Here we report on the reproducibility and enhanced accuracy of 2.5D ultra-short pulsed laser ablation of fused silica to structure complex optics by integrating centre recognition and height measurement within an automated machine setup and by sensitive adjustment of the applied laser parameters to optimize the ablated depth per path in multi-pass ablation processes. To exemplify the potential of these approaches, free-form optics and axicons are generated with improved geometrical and surface characteristics.

Keywords: Laserablation; Micro-Optics; Automation

1. Motivation

Ultrafast lasers are characterized by their ability to achieve high precision, short processing times, and a high degree of geometrical freedom due to the use of digital masking. It is evident that the manufacturing approach under consideration exhibits the necessary characteristics to fulfill the requirements of a wide range of processes, including drilling, cutting, and the ablation of materials of all material classes such as metals (Lutz et al. 2021), ceramics (Rung et al. 2021), polymers (Bischoff et al. 2022) and glasses (Yang et al. 2024).
With this approach, complex geometries can be produced by selective 2.5 D laser ablation. A second polishing step reduces surface roughness towards an optical surface quality, enabling the ablated geometries to be used in optical applications. In this context, nowadays, the demand for complex or non-rotation symmetric (freeform) optics is continuously rising. Due to the high degree of flexibility and high accuracy the combination of ultrafast lasers with CO_2 lasers meets the requirement of manufacturing of small optics for imaging purposes (Zubauskas et al. 2024; Blanco et al. 2015; Falaggis et al. 2022) or in laser manufacturing like an axicon for Bessel beam laser dicing (Dudutis et al. 2019).
Due to the high degree of precision required and the need for different laser sources, this manufacturing approach still requires operator-dependent positioning and process-dependent adjustments. As a result, the optics produced are associated with high costs that significantly exceed those of conventionally manufactured optics. In order to satisfy the criteria of an industrial-relevant process, it is imperative to enhance the throughput to minimize the individual costs per component. This objective can be achieved through the implementation of enhanced automation processes, while maintaining the stringent standards of precision required for the fabrication of optical components.
This study demonstrates the feasibility of maximizing accuracy in an automated process approach. For this purpose, the ablation per pass, which defines geometrical features and required angles as two of the most crucial parameters, is optimized with respect to reproducibility and quality. In particular, the geometrical lower angle limits of this approach are determined. By utilizing height measurement and center recognition, complex 2.5D geometries out of fused silica are produced in a fully automated laser micro ablation and the individual impact of the steps is characterized.

* Corresponding author.
E-mail address: Dominik.Muecke@th-ab.de.

2. Experimental setup and material

The material used in this study is natural fused silica (Type: EN08, GVB – Solutions in Glass, Germany). For the determination of ablated depth per pass, round specimens were used with a diameter of 50.8 +/- 0.5 mm and a thickness of 6 +/- 0.2 mm. Further experiments on the reproducibility of the center recognition and manufacturing of complex geometries were conducted on fused silica substrates with a diameter of 12.7 +/- 0.5 mm and a thickness of 2 +/- 0.2 mm. Both types are mechanically polished to a measured surface roughness (S_a) of 15 nm.

Experiments were conducted with the ultrafast laser (Carbide CB3-40W, Light Conversion, Lithuania) with a central wavelength of λ = 1030 nm and a tunable pulse duration which is, however, fixed to the lowest of 191 fs (FWHM) in this study. The integrated attenuation enables a precise variation of the needed pulse energy. Table 1 summarizes laser source and process parameters. The raw beam is enlarged by a motorized variable beam expander (HP-MEX 13, Optogama, Lithuania). The focusing is provide by a telecentric f-theta (Silverline, Jenoptik Optical Systems, Germany) with a focal length of 163 mm and positioned by galvanometric scanner head (Excelliscan 14, Scanlab, Germany). The resulting beam size was characterized by camera (UI-1490-SE-M-GL, IDS, Germany) with a pixel size of 1.67 µm as a focal diameter of 30 µm ($1/e^2$). Experimental setup is shown schematically in Figure 1.

Table 1. Overview of available laser- and processing parameters

Parameter		Unit
Wavelength	1030	nm
Polarization	Linear	
Pulse frequency rate	Single Shot – 2	MHz
Pulse duration	0.191 – 20	ps
Max. pulse energy	200	µJ
Spot size (1/e^2)	30 – 65	µm
Hatch overlap	73	%

Ablation of 2 mm x 2 mm cavities was performed to evaluate the necessary parameter combinations for a fixed ablated depth of 1 µm per pass, with a pulse frequency of 1000 kHz, a fixed hatch overlap of 73%, and a variable scan overlap, which can be calculated using the following equation:

$$P_O = 1 - \left(\frac{v_{scan}}{d_f * f_{rep}}\right) * 100\% \quad (1)$$

The following angle of the hatch is increased by a factor of 113° regarding the previous hatch direction to enhance quality due to changing scan paths. By varying the pulse energy E_p which is defined as:

$$E_p = P_{av} * f_{rep} \quad (2)$$

the ablated material per pass is adjusted. To guarantee equal optical properties during ablation and to reduce the minimal ablated depth per pass, the polished fused silica substrate (Kažukauskas et al. 2024) is laser roughened with a fluence of 2 J/cm^2 in combination with increased scan- and hatch overlap by a factor of 2 and thus increase the initial surface roughness to 290 nm.

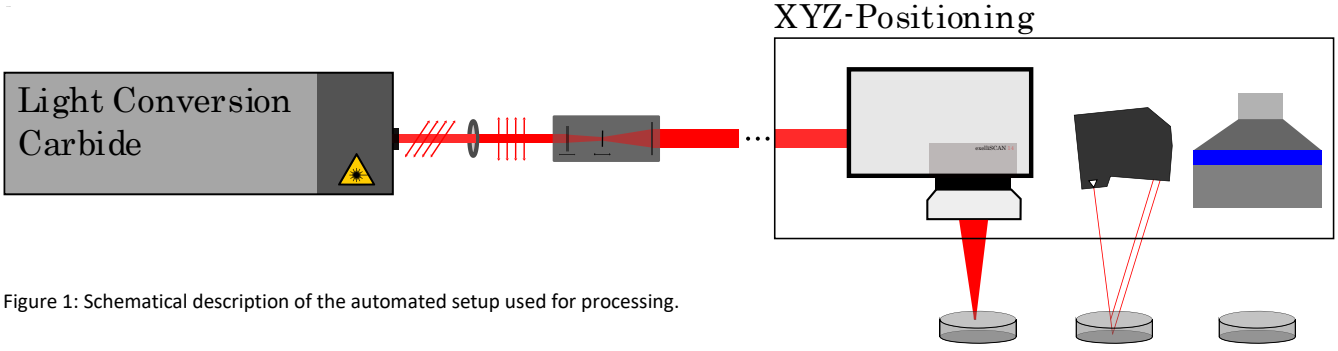

Figure 1: Schematical description of the automated setup used for processing.

The achievable accuracy is benchmarked by specimen individual alignment of focal plane and ablated depth (manual processing) which is measured by a laser scanning microscope (VK-X3000, Keyence, Japan). Standard deviation as a visualization of reproducibility of the ablation depth is calculated by a sample size of 12. By using the displacement sensor (LK-G5000, Keyence, Japan) with an accuracy of 2 µm, the distance between substrate and focal plane is measured and adjusted for the automated comparative study. Centering of the automated laser processing was performed by a centroid based approach (BHV Automation) using a telecentric objective and a CMOS camera (COB-123-M-USN-080-IR-C, Optoengineering, Italy) with a resolution of 4096 x 3000 pixels and a pixel size of 3.45 µm.

3. Results and Discussion

With respect to the laser ablation, different ablation depths are assured by a linear relation between ablated layer and performed laser ablation passes. Yet, depending on the required part accuracy, higher values can be achieved by an increased processing speed. However, due to the intention to produce high accuracy geometries for optical purposes, longer processing times can be accepted due to the need for a high demand of quality. To be able to meet these requirements a fixed ablation depth per pass of 1 µm was chosen which shows a sufficient quality. (Schwarz et al. 2018)

To produce 2.5D structures with a high accuracy in fused silica, the ablated depth per pass has to be constant at least down to the required depth of the ablation and must be adjusted by the processing parameters.

The energy input is varied by two different methods which are shown in Figure 2. Based on the experimental results of 100 ablation passes, the average depth per pass is identified. To find a suitable parameter for a fine adjustment, a variation of pulse energy and scanning speed is applied to compare the adjustment factor, which is defined as the function of the applied method to the ablation depth per pass to the performed increments.

With the minimal possible increment of the pulse energy method, shown in Figure 2 (a, c), the adjustment factor of 0.0042 µm/increment is identified. Differences in pulse energy are below the uncertainty of the measuring powermeter, repesenting calculative steps of 0.015 µJ per increment und thus equals a calculative pulseenergy of 10.455 µJ.

The utilization of the scanning speed at a fixed measured pulse energy of 10.4 µJ (1.47 J/cm^2) for fine-tuning shows an adjustment factor of 0.0024 µm/increment and such represents a more precise method of increasing the energy input. This enhancement is evident with a 57% smaller adjustement factor, which also shows lower fluctuations between the trendline. Whereas the variation of pulse energy resembles the minimal possible increments of the machine, the usage of the scanning speed would allow further 25000 increments within a single step of 25 mm/s performed.

The required ablation depth per pass should be adjusted on a macroscopic scale by the applied single pulse energy to maintain a high quality. Achieving a high accuracy in absolute ablation depth requires precise calibration with incremental adjustments made based on the scanning speed. This approach ensures the high constant quality of the ablation process, ensuring the precise execution of the procedure.

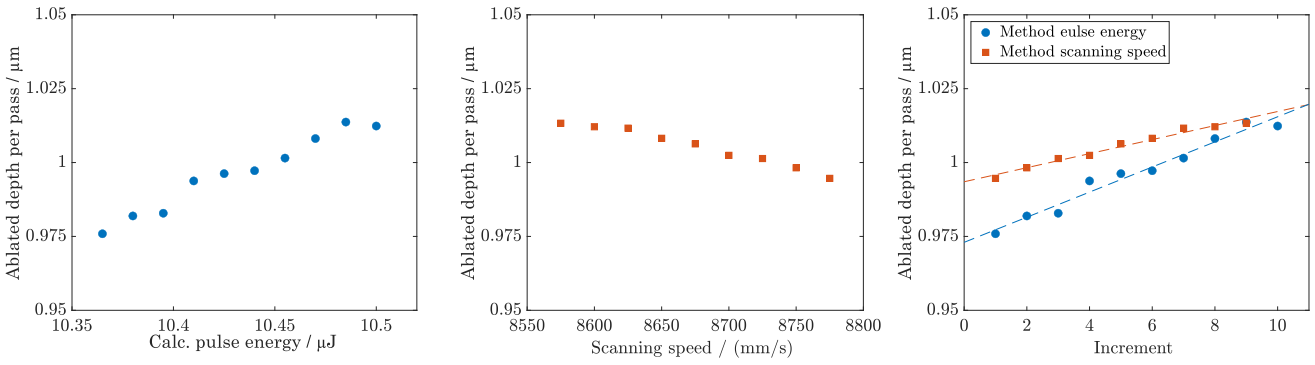

Figure 2: **(a)** Influence of pulse energy, **(b)** influence of applied scanning speed on the ablation per pass and in **(c)** the adjustment possibility based on the performed increments.

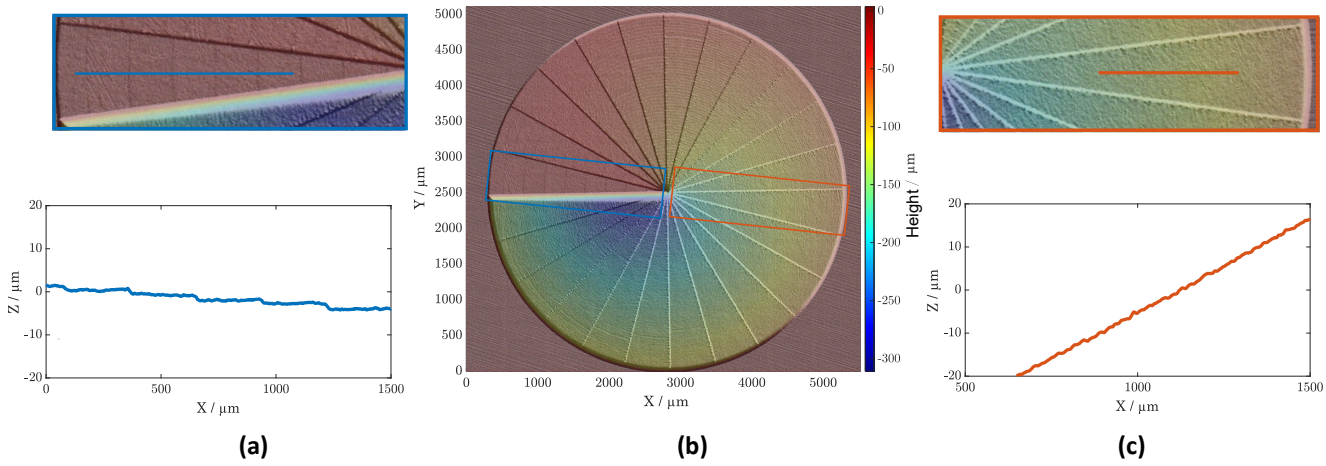

Figure 3: Overview of the Influence of 2.5D ablation angle from 0.2° to 4.8°shown in **(b). (a)** 0.2° **(c)** 2.6° representing magnified images and line profiles of the structures.

3.1 Dependency of ablation depth to translate angles

The generation of complex 2.5D structures by means of the layer by layer subtractive process is contingent upon the translation of the desired geometry into 2D slices. This is achieved by the division of the geometry into contours, which are then ablated by the previously evaluated parameters at a layerthickness of 1 µm. The implementation of different angles is achieved by employing different contours and by conducting a number of passes. For an application of complex shapes or freeform optics, it is necessary to transform the right depth at the needed position to ensure proper functionality and thus an accurate depth is crucial for a high quality. Additionally, it must be proven which angles can be translated by this ablation process. For this purpose, different angles were ablated in one file to evaluate the possible accuracy. Figure 3 (b) shows the variation of ideal angles between 0.2° and 4.8° in 0.2° steps.

Figure 3 (b) shows an overview of the experimental result on the ability to convert a constructed angle to ablated geometry. Regarding the smallest angle which is shown in detail in Figure 3 (a) with an angle of 0.2°, the measured value of 0.204° demonstrates the possible precision of this process. Nevertheless, small angles show stepped defects in the profile line. These steps occur because of the slight vertical distance over a long x-range with a step height of the ablated depth per pass of 1 µm. The number of passes required for this angle can be calculated by the length of the section and equals the number of steps in the ablation area. Increasing the angle by a factor of two results in an equal increase in the number of steps. By further increasing the angle, the steps morph together to a homogenous surface at an angle of 1.2°, visualized in detail by height and profileline of an angle of 2.6° in Figure 3 (c). Manufactured optical element can have defects if small

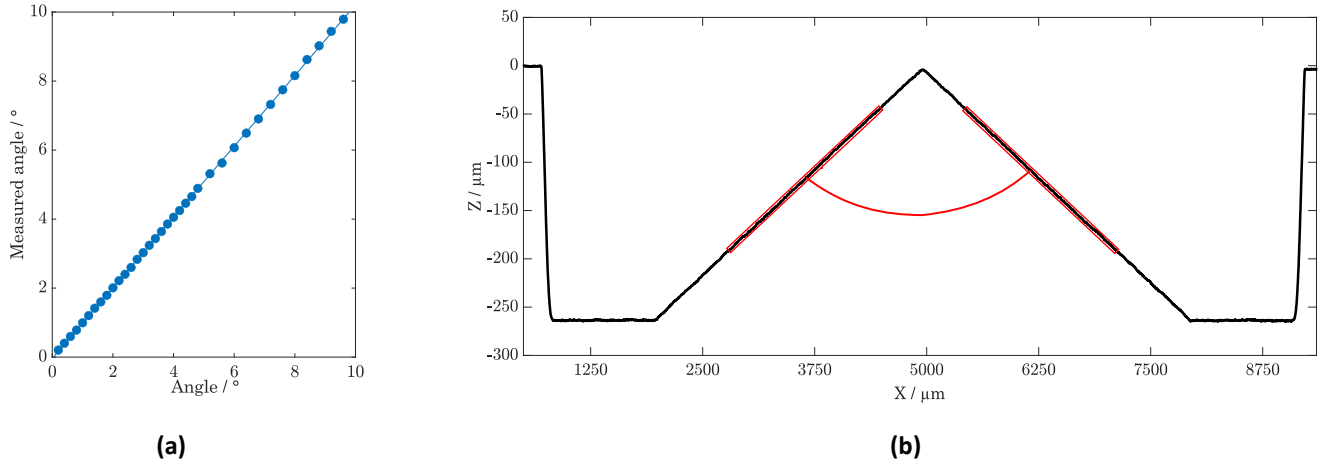

Figure 4: **(a)** visualization of the experimental results of the angle accuracy and **(b)** representative accuracy on axicon performed by manual processing with indication of tip angle measurment method.

angles are required. In this case, this effect can be reduced by an increased number of performed slices. Smaller values of the ablated depth per pass reduce the defects but increase the processing time due to smaller material removal rate. According to Figure 4 (a), the process can translate a required angle with identical processing parameter very accurately to the obtained geometry, which is visualized by a R^2 coefficient of the linear fit of 0.9999.
A complex optic – the Axicon - which can transform a gaussian beam into a Bessel beam distribution, which has already been proven as a suitable geometry for this hybrid manufacturing approach (Schwarz et al. 2018), is ablated to verify the ability to automate this ablation process. The Axicon to be ablated has an ideal flank angle of 10° which results in a tip angle of 170°. After 100 passes the focal plane is relatively shifted by the expected ablation depth of 100 µm, to ensure equal ablation circumstances during the process. Figure 4 (b) shows the profile line of the ablation and resembles a measured angle of 170.0°, which confirms the previsouly evaluated accuracy and also suggests a minor dependece on the geometry to be ablated.

3.2 Reproducibility influenced by defocusing

In an automated machine with multiple automation features, such as height measurement and image recognition, the degree of additional inaccuracy must be verified. Figure 5 (a) shows the achieved ablated depth of the cavity after identical ablation depth determination and (b) shows the resulting error to the mean ablation depth per pass to evaluate the reproducibility of automated laser processing in comparison to manual processing. According to Figure 5 (a), a fixed ablated depth per pass can be precisely adjusted independent of the applied functionalization. For manual processing an average ablation depth per 100 passes of 100.09 µm and for automated 99.78 µm which serves as a reference for evaluation of the resulting error, which is shown in Figure 5 (b). The lowest variation in ablation depth can be achieved with manual processing, which is attributed by a mean error of 0.06 µm (max: 0.17 µm, min: -0.24 µm). Automated processing leads to a slight increase of variation with equal parameters to a mean error of 0.19 µm (max: 0.32 µm; min: -0.43 µm), which can be positively influenced by focal position. By shifting the initial focal plane into the material by 50 µm to minimize the caustic-based influences, a reduced average statistically error of 0.11 µm (max: 0.26 µm; min: -0.30 µm) was achieved. For this reason, it is assumed that the accuracy will only deteriorate marginally because of automated processing.

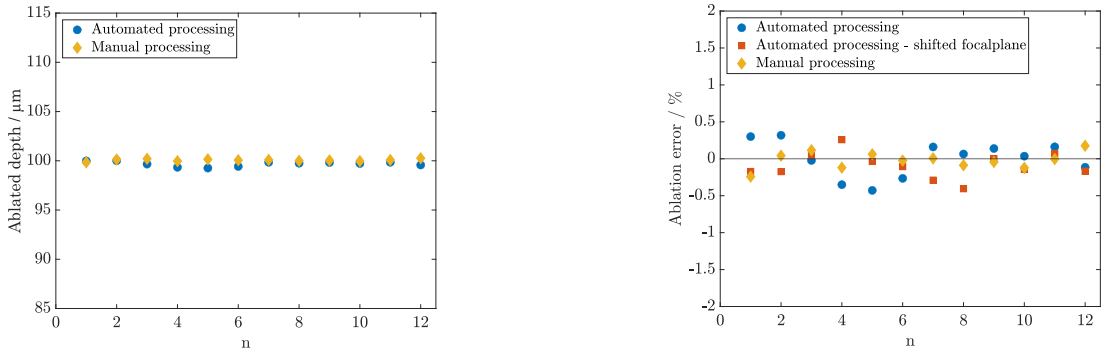

Figure 5: Influence of processing mode on the **(a)** achieved depth and **(b)** error with additionally shifting of the focal plane.

3.3 Automated centering

To be able to automate this ablation process besides the consistency in structural accuracy, the centering also plays a major role for optical components according to DIN ISO 10110-6. To provide the needed lateral centration on the raw glass substrate, the actual position is detected by the image recognition system and based on a centroid determination the offset between the center of the image recognition. The accuracy needed can be divided into two different factors. The first factor describes the actual centering of the structure on the overall glass substrate, which is attributed by a lateral offset of the processing head zero position in the center of the substrate. The experimental results indicate a mean error

of approximately 88.5 µm from the target circular center, resulting in an offset of 0.7% from the ideal measured diameter. Due to imperfections of the roundness of the initial substrate, the evaluated centroid is not set into center of a perfect circular shape which is why the centering of the substrate is considered as macroscopic centered.
A second factor of the centering is the reproducibility of the center within the automated process. For this evaluation a single substrate was height-, center measured 16 times and marked by crosses to evaluate the variation within an equal position. The center point of the crosses showed a maximal displacement of within a cycle diameter of 75 µm, which leads to centering of +/- 0.6 % on the base of the ideal diameter of the used silica substrate. The optical axis can be adjusted relative to the center of the substrate using adjustable optical mounts. If not applicable, centering can be improved to >1 µm by accurately measuring the optical axis and machining of the precision mount (Beier et al. 2012).

3.4 Automated manufacturing of optical high quality axicons

The quality of the automated processing is evaluated and divided into geometrical aspects, defined by the overall reproducibility of ablation and the accuracy of centering. Four optics have been produced to confirm previously suggested geometrical accuracy. All the ablated axicons show a very accurate angle of 170.0° which is the most critical quality factor for producing this particular optical element. Despite to the reference with a measured angular error of 0.01°, the automated processing shows a slight increase in to 0.08° which can mainly be attributed to the increased deviation of the ablation process shown in Figure 5 (b) and thus complicate the determination of a suitable parameter. Nevertheless, due to consistency in angular error, a second adjustment would be able to further minimize the error to reach the geometrical accuracy of manual processing. A comparison of manual and automated processing (Figure 6) reveals minimal differences in angular error. Automated processing does not negatively impact quality due to variations in geometrical accuracy, demonstrating the machine's possibility to consistently produce high-quality, complex optics.

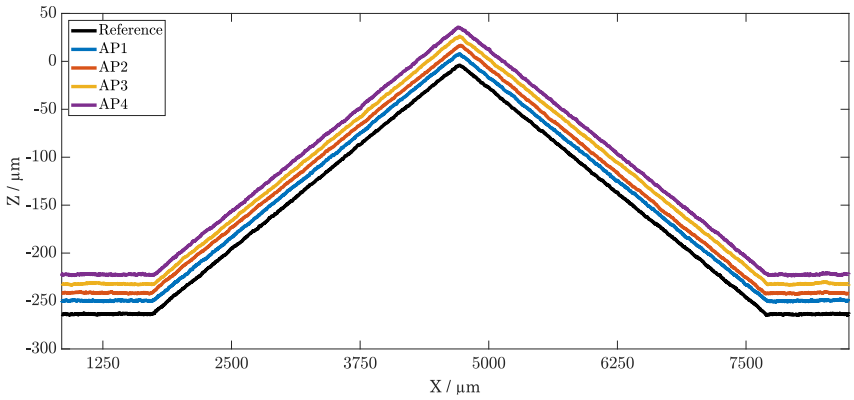

Figure 6: Ablation profiles of the manufactured axicons of the manual processing (MP) and automated processing (AP).

4. Conclusion

This contribution reports on the possibility to automate ablation of fused silica by utilizing height measurement, center recognition and process strategy. A two-step ablation per pass evaluation methodology, consisting of preliminary single pulse energy adjustment and subsequent fine adjustment by scanning speed, is demonstrated to ablate a fixed depth of 1 µm. Angles between 0.2° and 10° are confirmed as a possible way to translate a designed object into a 2.5D ablated geometry. Flatter angles than 1.2° show a very accurate angle with step defects which depend on the slicing parameters. Transferring manual to automated processing results in an increased mean error of the achieved ablation depth per pass which can be reduced by shifting the focal plane into the material. The centering process was divided into two distinct categories: macroscopic and reproducibility centering which was identified as a maximal circular offset of 0.7 % and 0.6 % of the used substrate diameter. The integration of centering height measurement and stable ablation demonstrates the capacity to generate multiple small optics without operator intervention. This advancement signifies a progression in the field of USP-laser processing and reflects a subsequent step toward an increased relevance of industrial manufacturing.

Acknowledgements

This research was funded by the Federal Ministry of Research, Technology and Space (BMFTR) within the project “ZDF-Laser” (13FH087IN0).

References

Beier, M., Gebhardt, A., Eberhardt, R., Tünnermann, A. 2012. Lens centering of aspheres for high-quality optics. aot 1 (6), 441–446.

Bischoff, K., Mücke, D., Roth, G.-L., Esen, C., Hellmann, Ralf 2022. UV-Femtosecond-Laser Structuring of Cyclic Olefin Copolymer. Polymers 14.

Blanco, M., Nieto, D., Flores-Arias, M. T. 2015. Fabrication of a microlens array in BK7 through laser ablation and thermal treatment techniques. Journal of Physics: Conference Series 605, 12023.

Dudutis, J., Stonys, R., Račiukaitis, G., Gečys, Paulius 2019. Glass dicing with elliptical Bessel beam. Optics & Laser Technology 111, 331–337.

Falaggis, K., Rolland, J., Duerr, F., Sohn, Alexander 2022. Freeform optics: introduction. Optics express 30 (4), 6450–6455.

Kažukauskas, E., Butkus, S., Jukna, V., Paipulas, Domas 2024. Surface roughness control in deep engraving of fused silica using femtosecond laser ablation. Surfaces and Interfaces 50, 104471.

Lutz, C., Roth, G.-L., Rung, S., Cemal, E. Hellmann, R. 2021. Efficient Ultrashort Pulsed Laser Processing by Dynamic Spatial Light Modulator Beam Shaping for Industrial Use. Journal of Laser Micro/Nanoengineering 16 (1).

Rung, S., Häcker, N., Hellmann, Ralf 2021. Thermal imaging of high power ultrashort pulse laser ablation of alumina towards temperature optimized micro machining strategies. IOP Conference Series: Materials Science and Engineering 1135 (1).

Schwarz, S., Rung, S., Esen, C., Hellmann, Ralf 2018. Fabrication of a high-quality axicon by femtosecond laser ablation and CO2 laser polishing for quasi-Bessel beam generation. Optics express 26 (18), 23287–23294.

Yang, Y., Bischoff, K., Mücke, D., Esen, C., Hellmann, Ralf 2024. UV-ultrashort pulsed laser ablation of fused silica. Journal of Laser Applications 36 (1).

Zubauskas, L., Markauskas, E., Vyšniauskas, A., Stankevič, V., Gečys, Paulius 2024. Comparative analysis of microlens array formation in fused silica glass by laser: Femtosecond versus picosecond pulses. Journal of Science: Advanced Materials and Devices 9 (4), 100804.